REFINEMENT OF LUNAR VIS/NIR PHASE CURVE ACQUIRED BY SELENE SPECTRAL PROFILER.
Y. Yokota[1], T. Matsunaga[2], M. Ohtake[1], J. Haruyama[1], R. Nakamura[3], S. Yamamoto[2], Y. Ogawa[4], T. Morota[1], C. Honda[4], K. Saiki[5], K. Nagasawa[5], K. Kitazato[4], S. Sasaki[6], A. Iwasaki[7], H. Demura[4], and N. Hirata[4], [1]Institute of Space & Astronautical Science, Japan Aerospace Exploration Agency, 3-1-1 Yoshinodai, Sagamihara, Kanagawa, Japan, (e-mail: yokota@planeta.sci.isas.jaxa.jp), [2]NIES, Japan, [3]AIST, Japan, [4] Univ. Aizu, [5]Osaka Univ., [6]NAOJ, [7]Univ. Tokyo.

Introduction: The SELENE Spectral Profiler (SP) acquired lunar visible to NIR spectral data at a spatial resolution of 500 m [1]. Photometric correction by an adequate phase curve is crucial for detailed analysis of the spectra. Many researchers (e.g., [2-7]) have investigated photometric correction of lunar data, but extensive study of wavelength coverage, geology dependence, and applicability for high-latitude regions, namely, observation at large incidence and phase angles, is still important.

Preliminary results of the lunar phase curve derived from SP data were reported in [8]. However, the target area was limited to a portion in the highlands, and regional material variation in that area was assumed to be negligible. Here we report refined results of the phase curves derived from SP data.

Model: Ideally, multiple observations in various geometry conditions are necessary to simultaneously decide all photometric parameters in a detailed model such as the Hapke model [9]. However, it is difficult to observe the entire lunar surface at various geometric conditions. Thus, an alternative empirical function is required. In this study, we followed the model of McEwen et al. [2, 3], which was proposed for Clementine photometric correction. The model function can be summarized as

$$r(\lambda;i,e,\alpha) = AX_L(i,e,\alpha)f(\lambda;\alpha) \quad , \qquad (1)$$

where i is incidence angle, e is emission angle, α is phase angle, r is the observed reflectance at wavelength λ and geometry (i,e,α), X_L is the Lunar-Lambert function for i- and e-dependence, $f(\alpha)$ is the phase function, and A is a constant that depends on albedo. We set the empirical coefficients in the Lunar-Lambert function the same as in [3].

For the phase function, we employed the following equations:

$$f(\alpha) = B(\alpha,h,B_0)P(\alpha,c,g_1), \qquad (2)$$

$$B(\alpha,h,b_0) = 1 + B_0[1+\tan(\alpha/2)/h], \qquad (3)$$

$$P(\alpha,c,g_1) = \frac{1-c}{2}p_{HG}(\alpha,g_1) + \frac{1+c}{2}p_{HG}(\alpha,-g_1), \qquad (4)$$

$$p_{HG}(\alpha,g_1) = \left(1-g_1^2\right)\Big/\left(1+g_1^2-2g_1\cos\alpha\right)^{3/2} \quad , \qquad (5)$$

where h, B_0, c, and g_1 are parameters determined by fitting to a dataset. Eq. (3) is the same as the shadow-hiding opposition effect (SHOE) function in the Hapke model. To describe function P, we chose a combination of two-term Henyey-Greenstein (2tHG) functions $p_{HG}(\alpha,g_1)$ (e.g. [10]). We chose it instead of the three-term HG function in [3], due to the limited phase-angle range in the SP observation. The parameters of the 2tHG can be converted into those of the 3tHG using g1 = -g2 and $F = (1+c)/2$.

The photometric correction to the standard viewing geometry (30°, 0°, 30°) is expressed as

$$r_{corr.}(30°,0°,30°) = r_{obs}(i,e,\alpha)\frac{X_L(30,0,30)}{X_L(i,e,\alpha)}\frac{f(30°)}{f(\alpha)} \quad . \qquad (6)$$

Data and Method: We used nearly 7000 orbits of SP data. One orbit contains over 10,000 spectra. The raw DN was converted to the radiance factor (RADF) by the procedures prepared for public release of SP data [11]. Since the radiometric calibration for longer wavelengths exceeding 1.6 μm remains incomplete, we use only the data at wavelengths shorter than 1645nm.

Albedo Classification. To derive $f(\alpha)$ from the observation, we needed a dataset that consist of relatively uniform albedo. To collect such data, we made a reference map by the SP 753nm band. Yokota et al. [6] demonstrated that the 750nm band phase curve of [3] can properly correct both highland and mare data at α=20–40°. We applied this phase curve to the SP 753nm band data in this phase angle range and made a reflectance map (Fig. 1) from the average in 1°×1° resolution tiles. The tentative albedo sub-group was defined as $r_{L,n+1}=r_{U,n}=[(1+0.015)/(1-0.015)]^{(n-1)}\times r_{L,1}$, where $r_{L,n}$ is the lower boundary reflectance of sub-group #n, and $r_{U,n}$ is the upper boundary reflectance of sub-group #n. We set $r_{L,1}$= 0.04, then all boundaries were defined systematically.

We excluded the tiles with a high (>0.1) $\sigma/r_{average}$ ratio. The distribution of groups for useful tiles thus became as depicted in Fig. 1. We defined the combined sub-groups #1 to #21 as the "Low albedo group" and the combined sub-groups #22 to #45 as the "High albedo group."

Filtering. Radiance factor data derived from those regions were divided by the X_L function. The observation geometry was calculated assuming that the Moon is a simple globe. We decided that the application of detailed topography data is a future issue. Alternatively, to statistically select the horizontal surface, we

introduced multi-stage filtering by a kind of median filter in each phase angle bin of 1° width [8].

Each sub-group data were normalized by the average of α=29.5–30.5°. The data were then merged into the low albedo group and the high albedo group.

Results and Discussion: Fig. 2 depicts the normalized phase curve plot at two representative bands. The observed phase curve plots were successfully derived from the SP data. Fitted curves are also shown in Fig. 4. Since the assessment of the coherent backscatter opposition effect is a difficult topic (e.g. [12, 13]), the data at α<5° were excluded from the fitting.

At large phase angle (α> ~80°), the observed data rapidly decreases with phase angle. This trend is difficult to describe by the 2tHG function. Thus, the data at α>75° were also excluded from the fitting. This trend is probably caused by the macroscopic roughness. We decided to prepare the additional method to treat this geometry range.

Fig. 3 shows the fitted parameters. Since the SHOE is caused by the single scattering, it is expected that the low albedo group exhibits steeper opposition surge than the high albedo group. Since the McEwen model does not treat single scattering and multiple scattering separately, the difference of the SHOE between the two albedo groups appears as the difference of B_0. Additionally, The parameter B_0 shows negative correlation with wavelength. This trend might be the reflection from the reddened feature of general lunar spectrum, that was caused by the space weathering.

The B_0 plot of the low albedo group shows a curve at ~1 μm. This wavelength range corresponds to the absorption bands of the mafic minerals those are abundant in lunar mare. Other parameters of the low albedo group also show curvatures at ~1 μm. In the high albedo group, the parameters h, g_1, c also show such features. However, the variation is smaller than the low albedo group.

References: [1] Matsunaga T. et al. (2008) *GRL*, 35, L23201. [2] McEwen A. S. (1996) *LPS XXVII*, Abstract p841. [3] McEwen A. S. et al. (1998) *LPS XXIX*, Abstract #1466. [4] Hillier J. K. et al. (1999) *Icarus*, 141, 205-225. [5] Kreslavsky M. A. et al. (2000) *JGR.*, 105 E8, 20,281-20,295. [6] Yokota Y. et al. (2003) *LPS XXXIV*, Abstract #1885. [7] Buratti et al. (2008) *LPS XXXIX*, Abstract #1471. [8] Yokota Y. et al. (2009) *LPS XL*, Abstract #2525. [9] Hapke, B. (1993), Theory of Reflectance and Emittance Spectroscopy, Cambridge Univ. Press, New York.. [10] Shepard, M. K., and P. Helfenstein (2007), JGR, 112, E03001. [11] Matsunaga et al. (2009), this issue. [12] Helfenstein et al. (1997), *Icarus*, 128, 2-14. [13] Shkratov et al. (1999), *Icarus*, 141, 132-155.

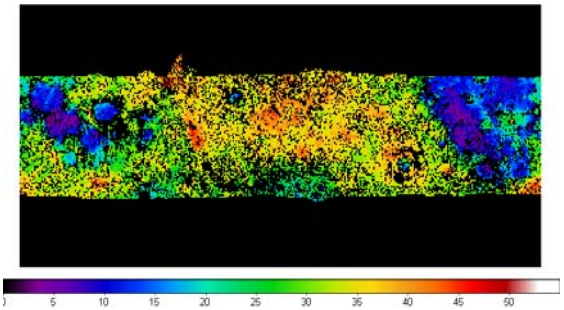

Fig. 1. Tentative albedo sub-groups. Projection method is Simple cylindrical. Left-most longitude is 0° E.

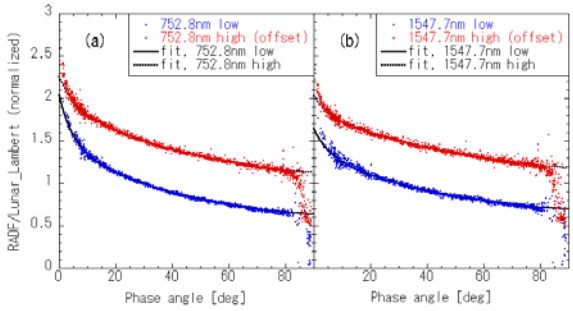

Fig. 2. Phase curve plot. Offset 0.5 was added to the high albedo group data. (a) 752.8 nm band. (b) 1547.8 nm band.

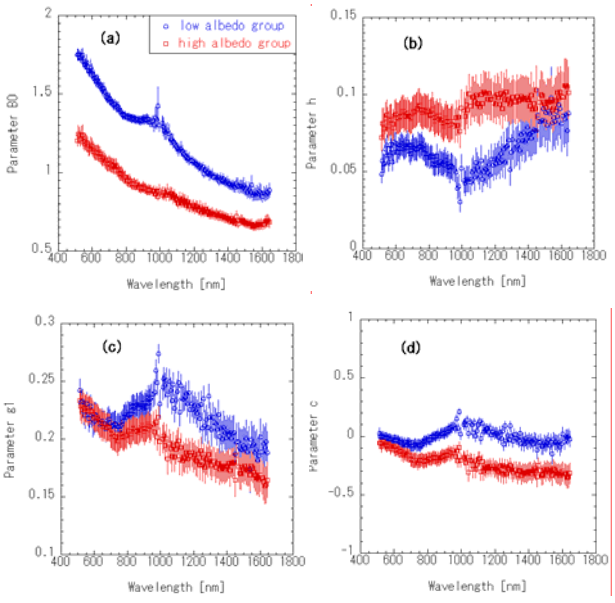

Fig. 3. Wavelength vs. phase function parameters. Error bars indicate fitting errors. (a) Parameter B_0. (b) Parameter h. (c) Parameter g_1. (d) Parameter c.